Shear buckling behaviour of welded stainless steel plate girders with transverse stiffeners

Article *in* Thin-Walled Structures · January 2018

DOI: 10.1016/j.tws.2017.10.043

6 authors, including:

Huanxin Yuan
Wuhan University
15 PUBLICATIONS **110** CITATIONS
SEE PROFILE

Jun Ye
University of Bath
11 PUBLICATIONS **14** CITATIONS
SEE PROFILE

Lu Yang
Beijing University of Technology
19 PUBLICATIONS **59** CITATIONS
SEE PROFILE

Chen XW, Yuan HX*, Du XX, Zhao Y, Ye J, Yang L. Shear buckling behaviour of welded stainless steel plate girders with transverse stiffeners. Thin-Walled Structures, 2018(122): 529-544.

Shear buckling behaviour of welded stainless steel plate girders with transverse stiffeners

X.W. Chen[a], H.X. Yuan[a, *], X.X. Du[a], Y. Zhao[a], J. Ye[b], L. Yang[c]

[a] *School of Civil Engineering, Wuhan University, Wuhan 430072, PR China*

[b] *Department of Architecture and Civil Engineering, University of Bath, Bath BA2 7AY, United Kingdom*

[c] *The College of Architecture and Civil Engineering, Beijing University of Technology, Beijing 100124, PR China*

Corresponding author:

Dr Huanxin Yuan, School of Civil Engineering, Wuhan University, Wuhan 430072, China. Email: yuanhx@whu.edu.cn

Abstract: The shear buckling behaviour of welded stainless steel plate girders with transverse stiffeners has been experimentally and numerically investigated in this paper. A total of seven plate girders with rigid/non-rigid end posts were fabricated from hot-rolled stainless steel plates, and each of the plate girders was subjected to a concentrated load at mid-span. The shear buckling characteristics and postbuckling behaviour were observed. Prior to testing, the initial local geometric imperfections and the material properties were accurately measured. The critical shear buckling strengths of the web plates were determined from the recorded surface strains and out-of-plane deflections, which were further compared with theoretically predicted values from elastic and inelastic assumptions. By using the general finite element (FE) software package ABAQUS, elaborated FE models were developed and validated against the obtained test results and other available existing test data. Upon validation of the FE models, parametric studies were subsequently carried out to explore the influences of initial local geometric imperfections, web aspect ratios, end post conditions, and material properties over a wide range of web slendernesses. The obtained test/FE results, together with other existing test data, were summarised to evaluate the current codified provisions in GB 50017, EN 1993-1-5, EN 1993-1-4, EN 1993-1-4+A1 and the design proposals from Estrada et al. Based on the test and numerical results, an alternative design approach that could account for the material non-linearity and rigid and non-rigid end posts has been proposed, which provides accurate and reasonable strength predictions for stainless steel plate girder with transverse stiffeners.

Keywords: Plate girders; Shear buckling; Stainless steel; FE modelling; Design method; Transverse stiffeners

1. Introduction

Due to the typical configuration of relatively slender web panels, the failure mode of shear buckling is of prominent importance in structural design of plate girders. Web stiffeners, including transverse and longitudinal stiffeners and occasionally inclined stiffeners, have been used to reinforce the web panel and therefore, significant increase of critical shear buckling strength can be achieved. Previous studies have been conducted to develop improved method for the prediction of shear buckling resistances [1-6], from which, it is well recognised that the critical shear buckling strength, postbuckling strength and frame action of the flanges and transverse stiffeners would contribute to the ultimate shear resistance of transversely stiffened plate girders. The existing design methods that applied to ordinary carbon steels are based primarily on the assumption of an idealised elastic, perfectly-plastic material behaviour. However, this idealisation may lead to inaccurate design of plate girders made of nonlinear metallic materials, including aluminium alloy and stainless steel [7]. Since the material properties of stainless steels vary significantly from those of carbon steels in terms of characteristics such as absence of yielding plateau and continuous strain hardening capacity, significant progress has been achieved in investigating the structural behaviour of stainless steel members under various loading conditions, and efficient design approaches have been proposed by many researchers [8-14].

The design and buckling behaviour of stainless steel plate girders subjected to shear failure have attracted attentions

in recent years. Olsson [15] conducted eight tests on austenitic and duplex stainless steel plate girders and established new design expressions for the calculation of shear resistance, which were later incorporated into the design code of EN 1993-1-4 [16]. Real et al. [17] presented an experimental programme of nine plate girders made of austenitic stainless steels. Their tests demonstrated the effect of material non-linearity on the shear strength. Meanwhile, Estrada et al. [18-20] performed comprehensive studies on austenitic stainless steel plate girders with transverse and longitudinal stiffeners. New design methods to determine the ultimate shear resistance of stainless steel plate girders were proposed subjected to complex boundary conditions. More recently, Saliba and Gardner [21,22] carried out nine tests on lean duplex stainless steel plate girders with rigid end posts, with a revised design approach for predicting the ultimate shear resistance presented. Numerical studies on shear buckling behaviour of stainless steel plate girders were also conducted by Hassanein [23,24], revealing the influences of the imperfections and the characteristics of failure mechanism. Despite the existence of experimental data, it may still be far from adequate to verify design approaches with reasonable accuracy due to the relatively high scatter in available test data. This is mainly due to the large family of stainless steel alloys pre-defined in various design codes. Therefore, the main aim of this paper is to investigate shear buckling and postbuckling behaviour and develop a uniform method for the design of welded stainless steel plate girders with transverse stiffener, crossing a wide variety of stainless steel alloys.

A total of seven transversely stiffened stainless steel plate girders were tested. The test specimens were loaded with concentrated load in the mid-span using simply-supported boundary conditions and they failed by shear buckling of the web. Based on the experimental results, numerical modelling on the shear buckling behaviour of the tested plate girders were performed in ABAQUS considering the measured imperfection and material nonlinearity, and the developed FE models were further validated against other available tests. A parametric study was carried out subsequently to examine the major factors affecting the ultimate shear resistance. The generated test and numerical results were used to assess the adequacy of design provisions in GB 50017 [25], EN 1993-1-5 [26], EN 1993-1-4 [16] and EN 1993-1-4+A1 [27] and the design expressions presented by Estrada et al. [19]. Finally, an alternative design approach taking into account the material non-linearity and rigid and non-rigid end posts were proposed, enabling a reasonably accurate and efficient prediction for ultimate shear resistances of stainless steel plate girders with transverse stiffeners. The research work presented in this study provides supplementary test data on stainless steel plate girders, and also contributes to the development of design recommendations for improvement on the first edition of Chinese design standard for structural stainless steel [28].

2. Test specimens

2.1 Specimen geometry

The test specimens include a group of seven girders, which were designed and fabricated from hot-rolled stainless steel plates. Both the austenitic grade EN 1.4301 (ASTM 304, GB/T S30408) and duplex grade EN 1.4462 (ASTM 2205, GB/T S22253) [29] were adopted in this study. By means of the laser cutting technique, the constitutive plates of each test specimen were cut in parallel to the longitudinal direction of hot-rolled coil. Compared to the water jet cutting, wire cutting and plasma arc cutting methods, the laser cutting technique provides a much more satisfactory cutting speed, quality and precision. Moreover, a relatively smaller amount of heat is introduced into the plates, resulting in negligible thermal distortions of flat plates during the operation process. Shielded metal arc welding (SMAW) using covered electrodes were performed to fabricate the I-section, where type E308 electrodes corresponded to the EN 1.4301 alloy and type E2209 electrodes to the EN 1.4462 alloy were used and all the electrodes were dried at 350 °C for one hour prior to welding [30]. Subsequent to welding, a hydraulic press with specially designed clamping apparatus successfully applied for fabricating built-up sections in the previous study [13], was also used to alleviate the residual distortions in the cross-sections.

Among the seven test specimens, five of them were designed with non-rigid end posts, while the other two with rigid end posts, as illustrated in Fig. 1. The average measured geometric dimensions are listed in Table 1, where $\overline{\lambda}_w$

is the web slenderness parameter defined in EN 1993-1-5, w_0 is the local imperfection amplitude measured with specially designed setup, and other symbols are defined with reference to Fig. 1. The specimens were labelled such that the material grade, cross-section dimensions and the end post condition can be readily recognised. For example, the label V-2205-R500ad1 defines a plate girder specimen made of EN 1.4462 alloy having rigid end posts, with nominal web 500 mm in depth and aspect ratio a/h_w=1.0. It is worth noting that all test specimens were designed to be slender cross-sections with Class 4 webs subject to bending stipulated in EN 1993-1-4+A1 [27].

2.2 Local geometric imperfections

Prior to member testing, the initial local geometric imperfections of the test specimens were measured. The adopted device and procedures for determining the geometric imperfections were similar to those presented by Yuan et al. [13], which were successfully applied for measurement of local imperfections in stainless steel built-up sections [31] and extruded aluminium alloy I-sections [32]. Furthermore, the digital linearly varying displacement transducer (LVDT) was replaced with a specially designed laser displacement sensor (LDS) to eliminate the possible frictional effects between the translational LVDT and the plate surface, as shown in Fig. 2. The LDS attached to the slide block of the guideway was driven by a magnetic stepping motor at a uniform translational speed of 20 mm/s along a specified path. Meanwhile, a constant data sampling rate of 20 Hz was used to generate one reading per millimeter. The measuring procedure was accomplished at three representative cross-sections of both panels for each specimen, as illustrated in Fig. 3, and the maximum value among the six cross-sections was taken as the local imperfection amplitude w_0 for the specimen. The measured imperfection distributions of the six cross-sections from specimen V-2205-500ad1.5 are plotted in Fig. 4, and the local imperfection amplitudes w_0 for all test specimens are summarised in Table 1. It can be seen from Table 1 that the maximum value of the local imperfection amplitude among all the specimens is 3.60 mm (h_w/139) for specimen V-304-500ad1.5.

2.3 Material properties

A series of tensile coupon tests were performed to obtain the material properties of the two stainless steel alloys. By using the wire-cutting technique, the standard tensile coupons of each alloy and each thickness were machined from the same hot-rolled stainless coil plates used to fabricate the specimens. Tensile coupons were cut from three directions, including the longitudinal (rolling direction), diagonal and transverse direction. Therefore, a total of forty-five tensile coupons involving fifteen different cases (as listed in Table 2) were tested, since three repeated coupons were prepared for each case. All tensile coupon tests were carried out by means of a 1000 kN capacity universal testing machine. The initial loading rate was set to be 0.5 mm/min until reaching the 0.6% strain limit, and it was gradually increased to 5 mm/min afterwards. Two orthogonal strain gauges and an extensometer were used to record the full stress-strain curves. The average measured material properties from the tested coupons are summarised in Table 2, where E_0 is the Young's modulus, v is the Poisson's ratio, $\sigma_{0.01}$, $\sigma_{0.2}$ and $\sigma_{1.0}$ are the 0.01%, 0.2% and 1.0% proof stresses, respectively. σ_u is the ultimate tensile stress. ε_u is the strain at the ultimate tensile stress (not obtained for EN 1.4301 coupons due to the limited range of the extensometer) and ε_f is the plastic strain at fracture based on elongation over the standard gauge length. n and m are the first and second strain hardening exponents, respectively, according to Annex C of EN 1993-1-4+A1 [27]. $n'_{0.2,1.0}$ is the strain hardening exponent from the modified two-stage Ramberg-Osgood model proposed by Gardner and Ashraf [7]. The ratios of 0.2% proof stresses (i.e., DT/LT and TT/LT) are also presented in Table 2, indicating the relatively small degree of anisotropy for the two stainless steel alloys. Specifically, the 0.2% proof stresses from the transverse coupons are generally higher than those from the longitudinal and diagonal coupons, and the maximum ratio is encountered for the EN 1.4462 coupons with nominal thickness of 4 mm in the transverse direction, where an increase of 16% in the 0.2% proof stress compared to the longitudinal direction is observed. It is also noted that the ultimate tensile strengths of the duplex grade EN 1.4462 are close to those of the austenitic grade EN 1.4301, while the latter alloy exhibited significantly lower nominal yield strengths but displayed more considerable strain hardening capacity. The typical full stress-strain curves for the two alloys are presented in Fig. 5, illustrating a nonlinear material behaviour.

3. Experimental programme

3.1 Test setup and instrumentation

The test setup is presented in Fig. 6, where the plate girders were subjected to a concentrated load at mid-span. The simply supported conditions were designed by using two bearings that were supported over the rigid steel pedestal. Each bearing was formed by a 60 mm diameter cylinder with polished surface. The bearing that was welded on a flat plate served as the pin support at one side, while the other was roller support without any welding, allowing for rotations and longitudinal displacements. Two pairs of small frames were clamped at each end of the tested specimens, where vertical and lateral displacements, and rotation about horizontal axis were restrained, as shown in Fig. 6(a). The small clamping frames were designed with two movable steel plates and adjustable bolts at each end, enabling restraints on plate girders with varying flange widths. A thin layer of lubricating oil was applied between the two plates and specimen to avoid the possible friction. Moreover, two lateral supports were provided by using a pair of triangular frames at each side of the plate girder with aspect ratio of 1.5 to prevent the specimen from lateral-torsional buckling failure.

The general instrumentation scheme of recording devices for the test specimens is presented in Fig. 7, which clearly provides the layout of the installed strain gauges and displacement transducers. A total of twenty triaxial (rosette) strain gauges were attached to both sides of the two web panels at critical points, monitoring the strain development of shear buckling. For each side of a web panel, three of the five triaxial strain gauges were placed along the centre of the panel, while the other two were located at the upper corner closing to the support, as shown in Fig. 7(a). Another twelve uniaxial strain gauges were installed at the upper flange and stiffeners where the plastic hinges might be formed to provide anchorage for the tension field. In addition, four uniaxial strain gauges were placed at the rigid end posts at each side for the two related plate girders to monitor the development of stress at the end posts, as shown in Fig. 7(a).

For the measurement of displacement, seven laser displacement sensors (LDSs) were also employed for each test specimen. Specifically, three LDSs were used to measure vertical displacements: one at mid-span and the other two at both supports. The other four LDSs were therefore located horizontally at the mid-height of each side of the web panels, recording the out-of-plane lateral displacements associated with the shear buckling.

The shear buckling tests were performed using a 5000 kN capacity hydraulic testing machine. The loading procedure was initially carried out by adopting load control at a rate of 0.2 kN/s. Once the shear buckling of web panels occurred, a displacement control was activated. A constant loading rate of 0.01 mm/s was applied afterwards, enabling the development and recording of the ultimate and post-peak response for each test specimen.

3.2 Test results

All seven tested plate girders were observed to fail by shear buckling and the deformed shapes are presented in Fig. 8, where the developed tension bands in web panels and the location (at the top and bottom flanges) of the plastic hinges can be observed. However, it should be mentioned that the experimental results of specimen V-304-500ad1 were lost due to the occurrence of an unexpected break-down of the testing machine.

The applied load versus mid-span vertical displacement curves are plotted in Fig. 9, where the curves of specimens with different aspect ratios and end post conditions are consistent in the initial stiffness, and then the response separated from each other due to the occurrence of shear buckling. The obtained ultimate shear resistances $V_{u,Test}$ of all tested specimens are presented in Table 3, and a comparison among the results will be discussed in the following subsections.

4. Analysis of the critical shear buckling strengths

4.1 Experimental strengths

Based on the recorded surface strains and lateral displacements of web panels, the critical shear buckling strengths can be determined [33,34]. Two experimental methods, namely the strain reversal method and the inflection point method, were introduced herein to acquire the critical shear buckling strengths. The initial part of the applied load versus principal surface strain curves (PT: principal tensile strain, PC: principal compressive strain) for specimen V-2205-R500ad1 are shown in Fig. 10, involving the six paired triaxial strain gauges attached on both web panels. The critical shear buckling strengths correspond to the reversal points where the principal compressive strain on the convex side of the buckled shape begins to decrease. Meanwhile, the load versus lateral displacement curves are plotted in Fig. 11, from which the critical shear buckling strengths corresponding to the inflection points can be obtained. It should be noted that the inflection points can be taken as bifurcation points of the measured lateral displacements by the two paired LDSs, and they are obtained by using the previously measured initial imperfection amplitude w_0, as shown in Fig. 11.

By adopting the two experimental methods, the critical shear buckling strengths $V_{cr,Test}$ and the corresponding shear buckling stresses $\tau_{cr,Test}$ ($=V_{cr,Test}/h_w t_w$) for all test specimens were obtained and summarised in Table 4, with theoretically predicted values of elastic and inelastic shear buckling stresses also presented. The calculation of the predicted values will be discussed in the succeeding subsections. It is worth noting that the minimum value of critical buckling strengths from different locations was taken as the critical shear buckling strength for both experimental methods. Compared with the results shown in Table 3, it can be seen that the shear buckling of web panels occurs at a load level which is lower than half of the peak load on average, indicating a considerable amount of postbuckling strength for each test specimen.

4.2 Predicted strengths

It is well-known that the elastic solution to the shear buckling stress $\tau_{cr,e}$ in a rectangular plate is given by:

$$\tau_{cr,e}=\kappa_\tau \frac{\pi^2 E}{12\left(1-\nu^2\right)}\left(\frac{t_w}{h_w}\right)^2 \tag{1}$$

in which κ_τ is the shear buckling coefficient, and it can be computed according to Eq. (2) for a plate simply supported on its four edges:

$$\kappa_\tau=\begin{cases}4.00+5.34/\alpha^2 & \text{for} \quad \alpha<1\\ 5.34+4.00/\alpha^2 & \text{for} \quad \alpha\geq 1\end{cases} \tag{2}$$

where the aspect ratio of web panel α is equal to a/h_w.

A comparison between the calculated elastic shear buckling stress $\tau_{cr,e}$ from Eq. (1) and the corresponding experimental values was performed, as illustrated in Table 4. It can be seen that the classical approach to shear buckling may lead to dramatically overestimated and scattered predictions due to the assumption of perfect elasticity. This difference indicates that it is necessary to take into account the material non-linearity of stainless steel alloys in the prediction of the shear buckling stress. The inelastic shear buckling stress of stainless steel plate can be obtained by introducing a plasticity reduction factor η.

$$\tau_{cr,p}=\eta\tau_{cr,e} \tag{3}$$

Regarding the calculation of the factor η for simply supported plate elements, two typical approaches that provided by ENV 1993-1-4 [35] and Real et al. [17] were considered herein, and the corresponding expressions are given by Eqs. (4) and (5), respectively:

$$\eta=G_t/G_0 \tag{4}$$

$$\eta=\sqrt{G_t/G_0} \tag{5}$$

where G_t and G_0 are the tangent and initial shear modulus respectively. Since the computation of G_t may require

iterative steps, simplified calculation methods were also provided by ENV 1993-1-4 [35] and Real et al [17].

Moreover, a newly revised expression derived by Estrada et al. [20] can be utilised to determine the inelastic shear buckling stress of stainless steel plate girders, accounting for both the material non-linearity and the practical boundary conditions of web panels:

$$\tau_{cr,p} = \eta \kappa_{rss} \frac{\pi^2 E}{12\left(1-\nu^2\right)}\left(\frac{t_w}{h_w}\right)^2 \tag{6}$$

where η is defined by Eq. (5) and κ_{rss} is the buckling coefficient.

Comparisons of the predicted critical shear buckling stresses by implementing these three approaches with the obtained experimental results are presented in Table 4. It is shown that the revised formula proposed by Estrada et al. [20] provided closer predictions of shear buckling stresses than the classical elastic approach, though very conservative shear buckling stresses were obtained. While the other two approaches introduced different plasticity reduction factors were able to provide more accurate strength predictions, which may be attributed to the appropriate consideration of the nonlinear material properties of stainless steel alloys.

5. Numerical modelling

5.1 Validation of the FE models

The general-purpose FE software package ABAQUS [36] was adopted to develop numerical models capable of simulating the shear buckling behaviour of stainless steel plate girders with transverse stiffeners. The numerical models can therefore be used to expand the available data for the development and validation of the succeeding proposed design method. The widely used four-node shell element S4R was employed to mesh the models, and the element edge dimension was taken as 15×15 mm in size based on a separate sensitivity analysis of computational efficiency and accuracy. The material properties obtained from the tensile coupon tests were used to define average stress-strain curves in FE models and then modelled by using the two-stage modified Ramberg-Osgood expressions proposed by Gardner and Ashraf [7]. Moreover, the obtained stress-strain model was converted into true stress versus true plastic strain prior to the material definition in ABAQUS. A linear eigenvalue buckling analysis was performed to generate the lowest relevant elastic buckling mode, which was therefore utilised as the initial geometric imperfection shape. By means of the *IMPERFECTION command, the measured amplitudes of imperfections were incorporated for subsequent FE analysis. It is worth noting that only the local geometric imperfections, were considered in the FE models. This is because lateral-torsional buckling was not observed in the tests with the additional lateral displacement constraints. Boundary conditions were carefully prescribed to reproduce the test setup. The clamped support conditions at both ends as well as the lateral supports, and the concentrated load at mid-span were all defined accordingly in the FE models, as illustrated in Fig. 12, where the symbols u_x, u_y and u_z represent displacements along with x, y and z axes, respectively, while θ_x, θ_y and θ_z are the corresponding rotations. The modified Riks method available in ABAQUS/standard was used in this study, enabling postbuckling analysis of the plate girder specimens.

The numerically predicted results derived from FE modelling were compared with the results obtained from tests. The accuracy of the FE models was assessed by comparing the load versus mid-span vertical displacement curves, shear buckling failure modes, principal membrane strains and the ultimate shear resistances. The typical comparison of load versus vertical displacement curves for specimen V-2205-500ad1.5 is presented in Fig. 13, and the corresponding failure modes are shown in Fig. 14, revealing nearly perfect agreement between FE and test results. The average ratio of FE predicted ultimate shear resistances to experimental values ($V_{u,FE}/V_{u,test}$) is 0.99 with a coefficient of variation (COV) of 0.01, as presented in Table 3 for all tested specimens. Furthermore, the principal membrane strains obtained from the attached triaxial strain gauges at the centre and upper corner of web panels exhibit close agreement with those extracted from the corresponding locations in the FE models, as displayed in Fig. 15, indicating the accurate predictions for the development of shear buckling in the web panels.

Meanwhile, other available test results were summarised and used to further validate the developed FE models. A total of thirty-four shear buckling tests on stainless steel plate girders were performed by Olsson [15], Real et al. [17], Estrada et al. [18] and Saliba and Gardner [21]. Thirteen of those were designed with rigid end posts, while the other twenty-one exhibited non-rigid end posts. Three different stainless steel grades, namely austenitic grade EN 1.4301, duplex grade EN 1.4462 and lean duplex grade EN 1.4162 were incorporated. The summarised thirty-four tests were therefore numerically modelled by means of the developed FE models in this paper. The comparison of the FE predicted ultimate shear capacities with all the test data is shown in Fig. 16. The mean value of $V_{u,FE}/V_{u,Test}$ is 0.99 with a COV of 0.06, revealing accurate and reliable estimation of ultimate shear capacities of all the tested plate girders. It is therefore concluded that the FE models are capable of accurately predicting the shear buckling behaviour of stainless steel plate girders, enabling the extension of the FE models to subsequent parametric studies.

5.2 Parametric analysis

Upon validation of the FE models, parametric studies were conducted involving a total of 468 plate girders. The influences of the major input parameters, including initial local geometric imperfections, web aspect ratios, end post conditions, and material properties were further explored over a wide range of web slendernesses. Since the numerically obtained ultimate shear resistances of plate girders consisted of contributions from both web and flanges, the web contributions, represented by the shear buckling factor χ_w, can be calculated by subtracting the flange contribution from the obtained ultimate shear resistance, which leads to:

$$\chi_w = \frac{V_u - V_{bf,Rd}}{h_w t_w \, f_{yw} / \sqrt{3}} \tag{7}$$

where f_{yw} is the yield strength of the web, and the contribution from flanges $V_{bf,Rd}$ is calculated by referring to the design provisions in EN 1993-1-5 with a modified distance c provided in EN 1993-1-4+A1, which will be discussed later.

Four different initial local imperfection amplitudes (b/100, b/200, b/300, b/500) of the web panel, were chosen to examine the imperfection sensitivity for shear buckling behaviour. The numerically predicted results for two stainless steel alloys are presented in Fig. 17, and it is shown that increasing the imperfection amplitudes has little effect on the web shear buckling factor for both austenitic and duplex plate girders. Therefore, the initial local imperfection amplitude b/200, corresponding to the recommendations set out in EN 1993-1-5, was adopted in the following parametric analysis.

It has been shown that the introduction of rigid end posts resulted in considerable increase in ultimate shear resistance of plate girders, as indicated in Section 3. A further analysis of the influence of rigid and non-rigid end posts was conducted, wherein six aspect ratios ranging from 0.75 to 3.0 were considered in numerical models. The comparison of the obtained FE results involving the two stainless steel alloys is shown in Fig. 18. It can be clearly seen that increased values of the web shear buckling factor were achieved by the application of rigid end posts, especially for the plate girders with higher web slenderness. This effect is more pronounced for web panels with smaller value of the aspect ratio. This is attributed to the fact that the plate girders with higher web slenderness developed more substantial postbuckling capacity due to the increased susceptibility to critical shear buckling. Meanwhile, a web panel with smaller value of the aspect ratio would benefit more from restraints provided by the rigid end posts. It is also shown in Fig. 18 that the plate girders made of duplex grade EN 1.4462 demonstrated lower values of the web shear buckling factor compared to those made of austenitic grade EN 1.4301, although it has been found that the former achieved higher ultimate shear resistance. The observed lower values of the web shear buckling factor of duplex plate girders can be resulted from the less developed strain hardening capacity of the material and, more importantly, the normalisation procedure where much higher nominal yield strength was applied. The differences in the web shear buckling factors between the two stainless steel alloys decreased with increasing values of the aspect ratio, revealing reduced influences from the material properties for the plate girder with larger web panels.

In the Ramberg-Osgood material model, the strain hardening exponent n and the non-dimensional proof stress

$e=\sigma_{0.2}/E_0$ are the two key material parameters that can characterise the stress-strain behaviour of different stainless steel alloys. The influence of material properties was analysed by taking four different values of exponent n (5, 7.5, 10, 16) and five values of parameter e (0.001, 0.0015, 0.002, 0.0025, 0.0035) as variables, covering the stainless steel grades included in EN 1993-1-4+A1 and Chinese code CECS 410. The results of the study to compare the effects of the two parameters are shown in Fig. 19 andFig. **20**. For a given parameter e, a smaller value of the strain hardening exponent n raises the web shear buckling factor due to the increased strain hardening capacity of the material, and this influence becomes more significant with increasing values of parameter e and web slenderness $\bar{\lambda}_w$. Moreover, increasing the non-dimensional proof stress e generally reduces the shear buckling factor, though higher ultimate shear resistances can be achieved, which can be attributed to the fact that the full utilisation of strength of the material may not be achieved.

6. Design methods for predicting ultimate shear resistance

6.1 General

All the previously available test data, along with the generated numerical results, were summarised to evaluate the design methods in GB 50017 [25], EN 1993-1-5 [26], EN 1993-1-4 [16] and EN 1993-1-4+A1 [27], and the design proposals presented by Estrada et al. [19]. A newly proposed alternative design approach that could account for the material non-linearity and rigid and non-rigid end posts was also assessed.

6.2 Evaluation of GB 50017

According to the Chinese code for design of carbon steel structures GB 50017 [25], the ultimate shear resistance V_u can be obtained from Eq. (8), which is based on the rotated stress field model developed by Höglund [37], yet the contribution from flanges is neglected:

$$V_u = \rho h_w t_w \frac{f_{yw}}{\sqrt{3}} \tag{8}$$

in which the shear reduction factor ρ can be obtained from Table 5, where the web slenderness λ_s corresponding to transversely stiffened plate girders can be calculated from Eq. (9) by introducing a material factor ε_k for stainless steel alloys [28], as given by Eq. (10). It is worth noting that the shear buckling coefficient κ_τ' can be obtained through multiplying the κ_τ defined according to Eq. (2) by a constant factor of 1.23, accounting for the effective restraints from flanges and transverse stiffeners.

$$\lambda_s = \frac{h_w/t_w}{37.4\varepsilon_k\sqrt{\kappa_\tau'}} = \frac{h_w/t_w}{41\varepsilon_k\sqrt{\kappa_\tau}} \tag{9}$$

$$\varepsilon_k = \sqrt{\frac{235}{f_{yw}}\frac{E_0}{206000}} \tag{10}$$

The comparison between the ultimate shear resistances predicted by GB 50017 and the summarised test/FE results is plotted in Fig. 21. The mean values of predicted strengths over test/FE capacity ratios are 0.79 and 0.84 for plate girders with rigid and non-rigid end posts, respectively, indicating relatively conservative strength predictions. The underestimated shear buckling strengths and the considerable scatter in the data are mainly due to the absence of the contribution from flanges in the prediction of ultimate strengths. In addition, the rigid and non-rigid end posts are not taken into account in GB 50017 [25], leading to insufficient prediction of the shear buckling capacities subjected to complex boundary conditions. Therefore, the necessity to take into account the contributions from flanges and the effect of rigid and non-rigid end posts has to be highlighted.

6.3 Evaluation of EN 1993-1-5 and EN 1993-1-4

The design approach adopted in EN 1993-1-5 [26] for predicting the shear resistance of carbon steel plate girders was also based on the rotated stress field model developed by Höglund [37]. The ultimate shear resistance contributed by the web panel and flanges is expressed as:

$$V_{\mathrm{b,Rd}} = V_{\mathrm{bw,Rd}} + V_{\mathrm{bf,Rd}} \le \frac{\eta f_{\mathrm{yw}} h_{\mathrm{w}} t_{\mathrm{w}}}{\sqrt{3}\gamma_{\mathrm{M1}}} \tag{11}$$

where the factor η is equal to 1.2, and γ_{M1} is the partial factor for member buckling and is set to unity in this study. The contribution from the web $V_{\mathrm{bw,Rd}}$ is defined as:

$$V_{\mathrm{bw,Rd}} = \frac{\chi_{\mathrm{w}} f_{\mathrm{yw}} h_{\mathrm{w}} t_{\mathrm{w}}}{\sqrt{3}\gamma_{\mathrm{M1}}} \tag{12}$$

in which the shear buckling factor χ_{w} should be obtained from Table 6, where the web slenderness $\overline{\lambda}_{\mathrm{w}}$ and material factor ε are defined by Eqs. (13) and (14), respectively.

$$\overline{\lambda}_{\mathrm{w}} = \frac{h_{\mathrm{w}}}{37.4 t_{\mathrm{w}} \varepsilon \sqrt{\kappa_{\tau}}} \tag{13}$$

$$\varepsilon = \sqrt{\frac{235}{f_{\mathrm{yw}}} \frac{E}{210000}} \tag{14}$$

Meanwhile, the contribution from the flanges $V_{\mathrm{bf,Rd}}$ is defined as:

$$V_{\mathrm{bf,Rd}} = \frac{b_{\mathrm{f}} t_{\mathrm{f}}^2 f_{\mathrm{yw}}}{c\gamma_{\mathrm{M1}}} \left(1 - \left(\frac{M_{\mathrm{Ed}}}{M_{\mathrm{f,Rd}}} \right)^2 \right) \tag{15}$$

in which M_{Ed} is the design bending moment, $M_{\mathrm{f,Rd}}$ is the moment of resistance of the cross section consisting of the effective area of the flanges only, and the distance between the positions of plastic hinges c can be calculated from the following expression:

$$c = a \left(0.25 + \frac{1.6 b_{\mathrm{f}} t_{\mathrm{f}}^2 f_{\mathrm{yf}}}{t_{\mathrm{w}} h_{\mathrm{w}}^2 f_{\mathrm{yw}}} \right) \tag{16}$$

Furthermore, Olsson [15] modified the design formulae in EN 1993-1-5 [26] by taking account of the contributions from the web and flanges. Specifically, the shear buckling factor χ_{w} was revised and is given in Table 7 for stainless steel plate girders with either rigid or non-rigid end posts, and the distance c can be calculated from Eq. (17). This design proposal has been incorporated into EN 1993-1-4 [16].

$$c = a \left(0.17 + \frac{3.5 b_{\mathrm{f}} t_{\mathrm{f}}^2 f_{\mathrm{yf}}}{t_{\mathrm{w}} h_{\mathrm{w}}^2 f_{\mathrm{yw}}} \right) \quad \text{and} \quad \frac{c}{a} \le 0.65 \tag{17}$$

Comparisons between the design strength curves predicted by EN 1993-1-5 [26] and EN 1993-1-4 [16] and the test/FE results are shown in Fig. 22. For the plate girders with rigid and non-rigid end posts, the average ratios of predicted to test/FE strengths are 0.89 and 0.81 from the design curves in EN 1993-1-5 [26], respectively, while the corresponding two average ratios are 0.74 and 0.79 according to those in EN 1993-1-4 [16]. It is shown that relatively more conservative strength predictions can be achieved by the EN 1993-1-4 design provisions, especially for the rigid end post condition, which is again due to the strengthening effects that have not been explicitly considered. Moreover, it should be noted that slightly unconservative predictions for plate girders with relatively small values of the web slenderness ($\overline{\lambda}_{\mathrm{w}} \le 1.0$) are achieved for both rigid and non-rigid end post conditions according to EN 1993-1-5 [26].

6.4 Evaluation of design proposals of Estrada et al. and EN 1993-1-4+A1

Revised design formulae were further developed by Estrada et al. [19] and Saliba et al. [22], and the web shear buckling factor χ_w was redefined in Table 8 and Table 9, respectively. The design proposal of Saliba et al. [22] has been incorporated into EN 1993-1-4+A1 [27]. In Estrada et al. [19] proposals, it can be noted that the rigid end post condition was not taken into account for web panels with aspect ratios higher than 1.0, and this was also not considered for web panels with the slenderness parameter smaller than 0.78. Therefore, on the basis of the EN 1993-1-4 [27] design provisions, the shear buckling resistance can be obtained by replacing the contribution from the web by inputting the two proposed web shear buckling factors (χ_w), together with the contribution from the flanges determined from Eqs. (15) and (17).

Fig. 23 presents the evaluation of the design strength curves of Estrada et al. and EN 1993-1-4+A1. Compared to the previously codified strength curves, a closer agreement between these curves and the summarised test/FE results with a lower scatter of the predictions is achieved due to the consideration of material non-linearity of stainless steel alloys and the end post conditions. Regarding the formulae proposed by Estrada et al., the mean value of strength ratios is 0.90 with a COV of 0.14 for plate girders with non-rigid end posts, while the corresponding mean strength ratio for rigid end post conditions is 0.93 with a COV of 0.10. Meanwhile, it is revealed that the average ratios of predicted to test/FE strengths from design curves of EN 1993-1-4+A1 are 0.88 for plate girders with non-rigid end post and 0.91 for rigid end post conditions, with corresponding COVs of 0.13 and 0.18, respectively. It may be concluded that the design curves of EN 1993-1-4+A1 provide good predictions on the ultimate capacity while maintaining a simple design process, but are slightly conservative on average, while the Estrada et al. proposals can lead to a slightly higher level of accuracy in predictions on average, but at the expense of more complicated formulae.

6.5 New design approach

The above comparisons show that the current design strength curves in GB 50017 are incapable of providing accurate predictions for stainless steel plate girders. Moreover, it is worth noting that the considerable postbuckling capacity is not established and exploited in the first Chinese specification for stainless steel structures CECS 410 [28]. Therefore, it is necessary to develop design approaches for the prediction of ultimate shear resistance of stainless steel plate girders. The evaluation of the existing design methods that accounted for contributions from both the web and flanges, has indicated that design provisions in EN 1993-1-5 [26] and EN 1993-1-4 [16] produce generally conservative predictions. It is also indicated that closer predictions can be obtained from EN 1993-1-4+A1 [27] and the revised formulae proposed by Estrada et al. [19], yet further improvement remains possible. Therefore, an alternative design approach considering the existing design methods will be proposed in this study.

Following the design procedure in EN 1993-1-4 [16], the ultimate shear resistance $V_{b,Rd}$ is taken as the summation of contributions from the web and flanges expressed in Eq. (11). The contribution from flanges $V_{bf,Rd}$ can still be obtained from Eq. (15), where the distance c given by Eq. (17) is adopted. Regarding the contribution from the web, the proposed revisions to the web shear buckling factor χ_w have been presented in Table 10, in which the web slenderness parameter λ_s should be calculated from Eq. (9), and the factor η is equal to 1.2, allowing for the exploitation of strain hardening in the case of stocky web panels. It can also be noted that the cases of rigid and non-rigid end post boundary conditions were separately considered in the proposed design approach.

The summarised test/FE results are compared with the strength predictions from the newly proposed design approach, as illustrated in Fig. 24. The average ratios of predicted strengths to test/FE results are 0.92 and 0.89 for plate girders with rigid and non-rigid end posts respectively, indicating the slightly conservative but close strength predictions. The average strength ratios and corresponding COVs of all the above design methods are tabulated in Table 11. Some scatter in the data can be observed for all the design methods, and this is mainly due to the differences in material properties of the stainless steel alloys considered, covering all the grades included in both the EN 1993-1-4+A1 [27] and the Chinese specification CECS 410 [28]. It is demonstrated that the proposed design method can be adopted as an alternative design approach, providing satisfactory strength predictions for stainless steel plate girders

with transverse stiffeners.

7. Conclusions

A comprehensive experimental and numerical investigation on shear buckling behaviour of stainless steel plate girders with transverse stiffeners has been performed in this study. A total of seven plate girders with rigid/non-rigid end posts fabricated from austenitic and duplex stainless steels were tested, failed by shear buckling of the web plate. The material properties of the two adopted stainless steel alloys and the initial local geometric imperfections were measured prior to the tests. The critical shear buckling stresses were experimentally determined by means of the attached strain gauges and the installed displacement transducers, which were further compared with theoretical values of elastic and inelastic shear buckling stresses.

Elaborate FE models, developed by using the ABAQUS software package, were validated against the obtained test results and other existing test data. Based upon the validated FE models, parametric studies were carried out to explore the major factors that have effects on the shear buckling capacity, including initial local geometric imperfections, web slendernesses and aspect ratios, end post conditions, and material properties. The generated test and FE results, along with the available test data, were used to assess the design provisions in GB 50017, EN 1993-1-5, EN 1993-1-4, EN 1993-1-4+A1 and design proposals presented by Estrada et al. It is shown that the design curves of GB 50017 leads to insufficient estimation of the shear buckling resistances due to the inadequate consideration of the contributions from flanges and the strengthening effects of rigid end posts. Meanwhile, the design provisions in both EN 1993-1-4 and EN 1993-1-5 were found to provide generally conservative predictions, while the design curves of EN 1993-1-4+A1 and Estrada et al. gave more accurate predictions for stainless steel plate girders with rigid/non-rigid end posts. Based on all the summarised test data and generated numerical results, an alternative design approach that could account for rigid and non-rigid end posts was proposed, covering all the stainless steel grades included in both EN 1993-1-4 and CECS 410. The evaluation of the proposed design method demonstrated the accuracy in predicting the shear buckling resistances of welded stainless plate girders with transverse stiffeners.

Acknowledgements

The financial support from the National Natural Science Foundation of China (Grant nos. 51508424 and 51478019), the China Postdoctoral Science Foundation (Grant no. 2015T80832), the Fundamental Research Funds for the Central Universities (Grant nos.2042017gf0047 and 2042016kf1125) are gratefully acknowledged by the authors. Very special thanks should be given to Mr Song Hu at Wuhan University for his kind help, and sincere thanks should also be extended to the technical staff in the Key Laboratory of Geotechnical and Structural Engineering Safety of Hubei Province, Wuhan University, for their technical support on the experimental work.

References

[1] K. Basler, Strength of plate girders in shear, J. Struct. Eng. ASCE 87 (ST7) (1961) 151–180.
[2] K.C. Rockey, M. Škaloud, The ultimate load behaviour of plate girders loaded in shear, Struct. Eng. 50 (1972) 29–48.
[3] G. Guarnieri, Collapse of plate girders with inclined stiffeners, J. Struct. Eng. ASCE 111 (2) (1985) 378–399.
[4] C.H. Yoo, S.C. Lee, Mechanics of web panel postbuckling behavior in shear, J Struct Eng. ASCE 132 (10) (2006) 1580–1589.
[5] M.M. Alinia, M. Shakiba, H.R. Habashi, Shear failure characteristics of steel plate girder, Thin-Walled Struct. 47 (2009) 1498-1506.
[6] D.W. White, M. G. Barker, Shear resistance of transversely stiffened steel I-girders, J. Struct. Eng. ASCE 134 (9) (2008) 1425–1436.
[7] L. Gardner, M. Ashraf, Structural design for non-linear metallic material, Eng. Struct. 28 (6) (2006) 926–934.
[8] K.J.R. Rasmussen, G.J. Hancock, Design of cold-formed stainless steel tubular members. I: Columns, J. Struct. Eng. ASCE 119 (8) (1993) 2349–2367.
[9] B. Young, W.M. Lui, Tests of cold-formed high-strength stainless steel compression members, Thin-Walled Struct. 44 (2) (2006) 224–234.
[10] L. Gardner, M. Theofanous, Discrete and continuous treatment of local buckling in stainless steel elements, J. Constr. Steel Res. 64 (11) (2008) 1207–1216.
[11] J. Becque, M. Lecce, K.J.R. Rasmussen, The direct strength method for stainless steel compression members, J. Constr. Steel Res. 64 (11) (2008) 1231–1238.

[12] M. Theofanous, L. Gardner, Experimental and numerical studies of lean duplex stainless steel beams, J. Constr. Steel Res. 66 (6) (2010) 816–825.
[13] H.X. Yuan, Y.Q. Wang, Y.J. Shi, L. Gardner, Stub column tests on stainless steel built-up sections, Thin-Walled Struct. 83 (2014) 103–114.
[14] L. Gardner, Y.D. Bu, M. Theofanous, Laser-welded stainless steel I-sections: Residual stress measurements and column buckling tests, Eng. Struct. 127 (2016) 536–548.
[15] A. Olsson, Stainless steel plasticity-material modeling and structural application [PhD dissertation], Lulea University of Technology, Sweden, 2001.
[16] EN 1993-1-4, Eurocode 3: Design of steel structures–Part 1.4: General rules–supplementary rules for stainless steel, CEN, 2006.
[17] E. Real, E. Mirambell, I. Estrada, Shear response of stainless steel plate girders, Eng. Struct. 29 (7) (2007) 1626–1640.
[18] I. Estrada, E. Real, E. Mirambell, General behaviour and effect of rigid and non-rigid end post in stainless steel plate girders loaded in shear. Part I: Experimental study, J. Constr. Steel Res. 63 (7) (2007) 970–984.
[19] I. Estrada, E. Real, E. Mirambell, General behaviour and effect of rigid and non-rigid end post in stainless steel plate girders loaded in shear. Part II: Extended numerical study and design proposal, J. Constr. Steel Res. 63 (7) (2007) 985–996.
[20] I. Estrada, E. Real, E. Mirambell, Shear resistance in stainless steel plate girders with transverse and longitudinal stiffening, J. Constr. Steel Res. 64 (11) (2008) 1239–1254.
[21] N. Saliba, L. Gardner, Experimental study of shear response of lean duplex stainless steel plate girders, Eng. Struct. 46 (2013) 375–391.
[22] N. Saliba, E. Real, L. Gardner, Shear design recommendations for stainless steel plate girders, Eng. Struct. 59 (2014) 220–228.
[23] M.F. Hassanein, Imperfection analysis of austenitic stainless steel plate girders failing by shear, Eng. Struct. 32 (3) (2010) 704–713.
[24] M.F. Hassanein, Finite element investigation of shear failure of lean duplex stainless steel plate girders, Thin-Walled Struct. 49 (8) (2011) 964–973.
[25] GB 50017-2003, Code for Design of Steel Structures, China Planning Press, Beijing, 2003 (in Chinese).
[26] EN 1993-1-5, Eurocode 3: Design of steel structures–Part 1.5: Plated structural elements, CEN, 2006.
[27] EN 1993-1-4+A1, Eurocode 3: Design of steel structures–Part 1.4: General rules–supplementary rules for stainless steel, CEN, 2015.
[28] CECS 410:2015, Technical specification for stainless steel structures, China Planning Press, Beijing, 2015 (in Chinese).
[29] GB/T 20878-2007, Stainless and heat-resisting steel–Designation and chemical composition, Standards Press of China, Beijing, 2007 (in Chinese).
[30] GB/T 983-2012, Stainless steel covered electrodes, Standards Press of China, Beijing, 2012 (in Chinese).
[31] H.X. Yuan, Y.Q. Wang, L. Gardner, Y.J. Shi, Local-overall interactive buckling of welded stainless steel box section compression members, Eng. Struct. 67 (2014) 62–76.
[32] H.X. Yuan, Y.Q. Wang, T. Chang, X.X. Du, Y.D. Bu, Y.J. Shi, Local buckling and postbuckling strength of extruded aluminium alloy stub columns with slender I-sections, Thin-Walled Struct. 90 (2015) 140–149.
[33] W.P. Vann, J. Sehested, Experimental techniques for plate buckling, in: Proceedings of the 2nd specialty conference on cold-formed steel structures, University of Missouri-Rolla, USA, October, 1973.
[34] K.R. Venkataramaiah, J. Roorda, Analysis of local plate buckling experimental data, in: Proceedings of the 6th international specialty conference on cold-formed steel structures, University of Missouri-Rolla, USA, November, 1982.
[35] ENV 1993-1-4, Eurocode 3: design of steel structures–part 1.4: general rules–supplementary rules for stainless steels, CEN, 1996.
[36] H. Hibbitt, B. Karlsson, P. Sorensen, ABAQUS Analysis User's Manual Version 6.10, Dassault Systèmes Simulia Corp.: Providence, RI, USA, 2011.
[37] T. Höglund, Shear buckling resistance of steel and aluminium plate girders, Thin-Walled Struct. 29 (1–4) (1998) 13–30.

Table 1

Average measured geometric dimensions for plate girders

Plate girder	Material grade	L	a	e	h_w	b	t_w	t_f	t_s	$\bar{\lambda}_w$	w_0
V-304-300ad1	1.4301	798.8	299.2	100.2	299.5	134.0	3.82	11.85	11.85	0.794	0.46
V-304-500ad1	1.4301	1197.8	498.8	100.1	498.4	150.0	3.82	11.85	11.85	1.323	1.45
V-304-500ad1.5	1.4301	1696.6	747.6	100.7	498.6	150.2	4.11	11.85	11.85	1.409	3.60
V-304-R500ad1	1.4301	1198.2	499.0	100.1	498.6	150.0	4.11	11.85	11.85	1.230	1.44
V-2205-500ad1	1.4462	1198.3	499.0	100.2	498.4	150.2	3.90	12.59	12.59	1.721	0.75
V-2205-500ad1.5	1.4462	1698.3	748.7	100.4	499.4	150.1	3.90	12.59	12.59	1.972	1.24
V-2205-R500ad1	1.4462	1198.9	498.7	100.8	498.9	150.1	3.90	12.59	12.59	1.721	1.19

All dimensions except the nondimensional slenderness parameter $\bar{\lambda}_w$ are in mm.

Table 2

Average measured material properties from tensile coupon tests

Grade	t (mm)	Direction[a]	E_0 (MPa)	v	$\sigma_{0.01}$ (MPa)	$\sigma_{0.2}$ (MPa)	$\sigma_{1.0}$ (MPa)	σ_u (MPa)	ε_u (%)	ε_f (%)	Exponents			Anisotropic ratio
											n	m	$n'_{0.2,1.0}$	
		LT	193500	0.242	237.4	289.2	326.4	783.9	-	64.2	15.2	2.3	1.7	-
1.4301	3.82	DT	191200	0.257	239.5	289.4	329.8	790.3	-	62.0	15.9	2.3	1.7	1.00
		TT	192100	0.241	235.0	289.2	333.2	794.1	-	58.3	14.5	2.3	1.7	1.00
		LT	189000	0.251	192.3	279.7	316.8	756.3	-	69.5	8.0	2.3	2.2	-
1.4301	4.11	DT	188000	0.258	229.8	289.8	330.1	752.2	-	62.7	12.9	2.3	1.8	1.04
		TT	194600	0.258	228.8	295.1	336.6	764.4	-	63.1	11.8	2.4	1.9	1.06
		LT	182800	0.258	184.7	280.4	319.1	719.6	-	57.7	7.2	2.4	2.4	-
1.4301	11.85	DT	186600	0.290	194.3	285.3	326.6	724.8	-	57.0	7.8	2.4	2.3	1.02
		TT	186900	0.277	208.2	292.5	334.8	738.0	-	54.1	8.8	2.4	2.2	1.04
		LT	204800	0.228	345.3	539.6	604.1	761.4	26.1	40.2	6.7	3.5	3.3	-
1.4462	3.90	DT	190100	0.295	325.8	536.7	613.7	747.0	27.3	42.7	6.0	3.5	3.7	0.99
		TT	224600	0.225	425.7	626.8	692.0	829.9	19.5	34.2	7.9	3.6	3.1	1.16
		LT	184000	0.226	227.8	464.6	552.8	705.3	23.3	37.4	4.2	3.3	4.4	-
1.4462	12.59	DT	174000	0.266	203.2	455.5	551.3	696.0	24.2	40.5	3.7	3.3	4.9	0.98
		TT	202000	0.240	207.7	502.6	598.0	748.0	20.9	32.6	3.4	3.3	5.0	1.08

[a] LT: longitudinal tension, DT: diagonal tension, TT: transverse tension

Table 3

Comparison of ultimate shear resistance between test and FE results

Plate girder	$\bar{\lambda}_w$	$V_{u,Test}$ (kN)	$V_{u,FE}$ (kN)	$V_{u,FE}/V_{u,Test}$
V-304-300ad1	0.794	253.2	246.3	0.97
V-304-500ad1	1.323	-	270.0	-
V-304-500ad1.5	1.409	243.2	240.8	0.99
V-304-R500ad1	1.230	322.2	315.6	0.98
V-2205-500ad1	1.721	453.9	458.4	1.01
V-2205-500ad1.5	1.972	385.9	387.0	1.00
V-2205-R500ad1	1.721	512.7	507.2	0.99
Mean	-	-	-	0.99
COV	-	-	-	0.01

Table 4

Critical shear buckling strengths of the test specimens

Plate girder	Experimental results				Elastic shear buckling stress ($\tau_{cr,e}/\tau_{cr,Test}$)	Inelastic shear buckling stress ($\tau_{cr,p}/\tau_{cr,Test}$)		
	Based on surface strains		Based on lateral deflections			ENV 1993-1-4 [35]	Real et al. [17]	Estrada et al. [20]
	$V_{cr,Test}$ (kN)	$\tau_{cr,Test}$ (MPa)	$V_{cr,Test}$ (kN)	$\tau_{cr,Test}$ (MPa)				
V-304-300ad1	161	140.5	192	167.5	1.89	0.75	0.86	1.00
V-304-500ad1	-	-	-	-	-	-	-	-
V-304-500ad1.5	131	63.7	153	74.5	1.32	1.05	1.08	1.34
V-304-R500ad1	153	74.5	176	85.6	1.48	1.03	1.08	1.25
V-2205-500ad1	168	86.2	170	87.2	1.22	1.14	1.14	1.32
V-2205-500ad1.5	127	65.1	116	59.5	1.23	1.23	1.21	1.51
V-2205-R500ad1	160	82.1	155	79.5	1.28	1.20	1.20	1.39
Mean	-	-	-	-	1.40	1.07	1.09	1.30
COV	-	-	-	-	0.25	0.17	0.13	0.17

Table 5

The shear reduction factor ρ in Chinese code GB 50017 [25]

λ_s	Rigid and non-rigid end posts
$\lambda_s \le 0.8$	1
$0.8 < \lambda_s \le 1.2$	$1-0.5(\lambda_s-0.8)$
$\lambda_s > 1.2$	$1/\lambda_s^{1.2}$

Table 6

The shear buckling factor χ_w according to EN 1993-1-5 [26]

$\bar{\lambda}_w$	Rigid end post	Non-rigid end post
$\bar{\lambda}_w < 0.83/\eta$	η	η
$0.83/\eta \le \bar{\lambda}_w < 1.08$	$0.83/\bar{\lambda}_w$	$0.83/\bar{\lambda}_w$
$\bar{\lambda}_w \ge 1.08$	$1.37/\left(0.7+\bar{\lambda}_w\right)$	$0.83/\bar{\lambda}_w$

Table 7

The shear buckling factor χ_w according to EN 1993-1-4 [16]

$\bar{\lambda}_w$	Rigid and non-rigid end posts
$\bar{\lambda}_w \le \frac{0.6}{\eta}$	η
$\bar{\lambda}_w > \frac{0.6}{\eta}$	$0.11+\frac{0.64}{\bar{\lambda}_w}-\frac{0.05}{\bar{\lambda}_w^{\,2}}$

Table 8

The shear buckling factor χ_w proposed by Estrada et al. [19]

Aspect ratio	$\bar{\lambda}_w$	Rigid end post	Non-rigid end post
$a/h_w \le 1.0$	$\bar{\lambda}_w \le 0.38$	1.2	1.2
	$0.38 < \bar{\lambda}_w \le 0.78$	$0.48+\frac{0.35}{\bar{\lambda}_w}-\frac{0.03}{\bar{\lambda}_w^{\,2}}$	$0.48+\frac{0.35}{\bar{\lambda}_w}-\frac{0.03}{\bar{\lambda}_w^{\,2}}$
	$\bar{\lambda}_w > 0.78$	$0.48+\frac{0.35}{\bar{\lambda}_w}-\frac{0.03}{\bar{\lambda}_w^{\,2}}$	$0.33+\frac{0.55}{\bar{\lambda}_w}-\frac{0.095}{\bar{\lambda}_w^{\,2}}$
$a/h_w > 1.0$	$\bar{\lambda}_w \le 0.47$	1.2	1.2
	$\bar{\lambda}_w > 0.47$	$0.2+\frac{0.6}{\bar{\lambda}_w}-\frac{0.06}{\bar{\lambda}_w^{\,2}}$	$0.2+\frac{0.6}{\bar{\lambda}_w}-\frac{0.06}{\bar{\lambda}_w^{\,2}}$

Table 9

The shear buckling factor χ_w according to EN 1993-1-4+A1 [27]

$\bar{\lambda}_w$	Rigid end post	Non-rigid end post
$\bar{\lambda}_w \le 0.65/\eta$	η	η
$0.65/\eta < \bar{\lambda}_w < 0.65$	$0.65/\bar{\lambda}_w$	$0.65/\bar{\lambda}_w$
$\bar{\lambda}_w \ge 0.65$	$1.56/(0.91+\bar{\lambda}_w)$	$1.19/(0.54+\bar{\lambda}_w)$

Table 10

Proposed web shear buckling factor χ_w

λ_s	Rigid end post	Non-rigid end post
$\lambda_s \le \frac{0.60}{\eta}$	η	η
$\frac{0.60}{\eta} < \lambda_s < 0.70$	$0.12+\frac{0.80}{\lambda_s}-\frac{0.13}{\lambda_s^2}$	$0.6/\lambda_s$
$\lambda_s > 0.70$	$0.12+\frac{0.80}{\lambda_s}-\frac{0.13}{\lambda_s^2}$	$0.12+\frac{0.72}{\lambda_s}-\frac{0.14}{\lambda_s^2}$

Table 11

Comparison of strength prediction ratios (Predicted/Test(FE)) for the considered design methods and proposals

	Existing design methods/proposals										New proposals	
	GB 50017		EN 1993-1-5		EN 1993-1-4		Estrada et al.		EN 1993-1-4+A1			
	Non-rigid	Rigid	Non-rigid	Rigid	Non-rigid	Rigid	Non-rigid	Rigid	Non-rigid	Rigid	Non-rigid	Rigid
Mean	0.84	0.79	0.81	0.89	0.79	0.74	0.92	0.90	0.88	0.92	0.89	0.92
COV	0.25	0.28	0.17	0.16	0.10	0.13	0.10	0.09	0.12	0.14	0.10	0.15

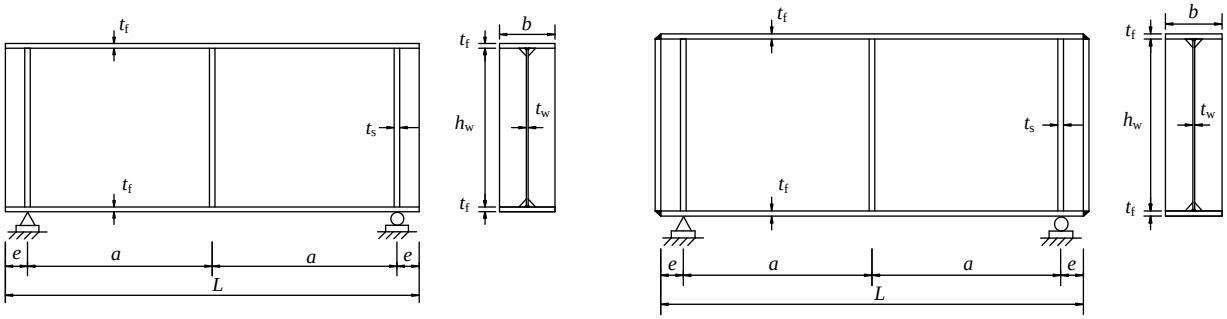

(a) Non-rigid end post (b) Rigid end post

Fig. 1. Geometry of the test specimens

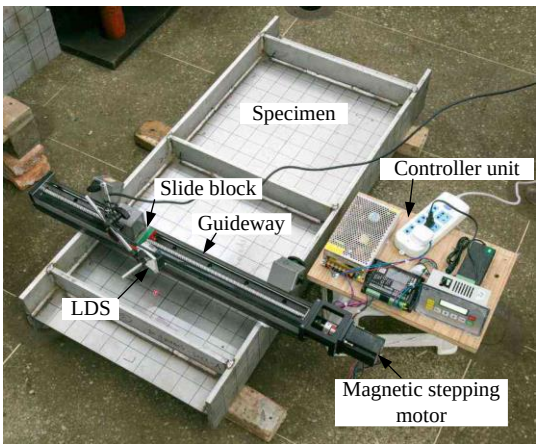

Fig. 2. Measurement of local geometric imperfections

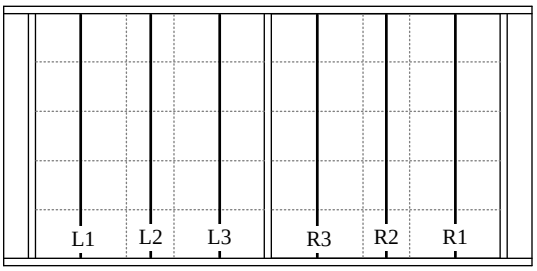

Fig. 3. Location of measured cross-sections

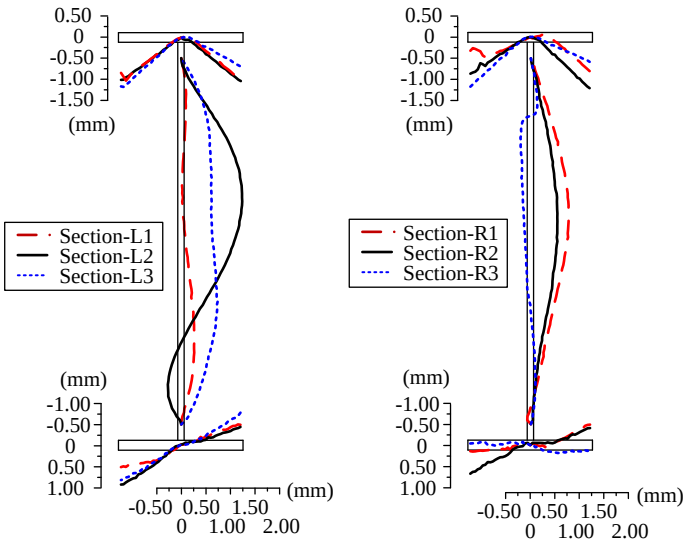

Fig. 4. Measured local imperfection distribution for specimen V-2205-500ad1.5

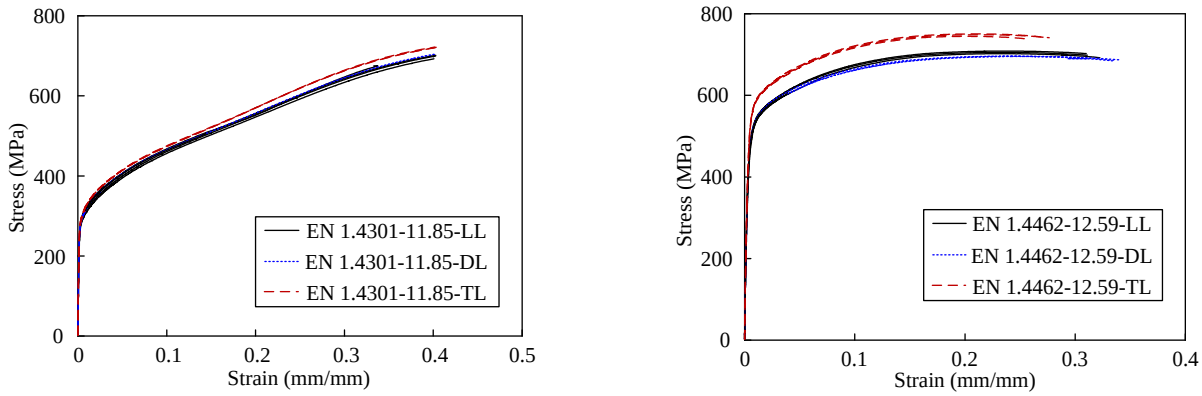

(a) Austenitic grade EN 1.4301 (b) Duplex grade EN 1.4462

Fig. 5. Stress-strain curves of the tensile coupons

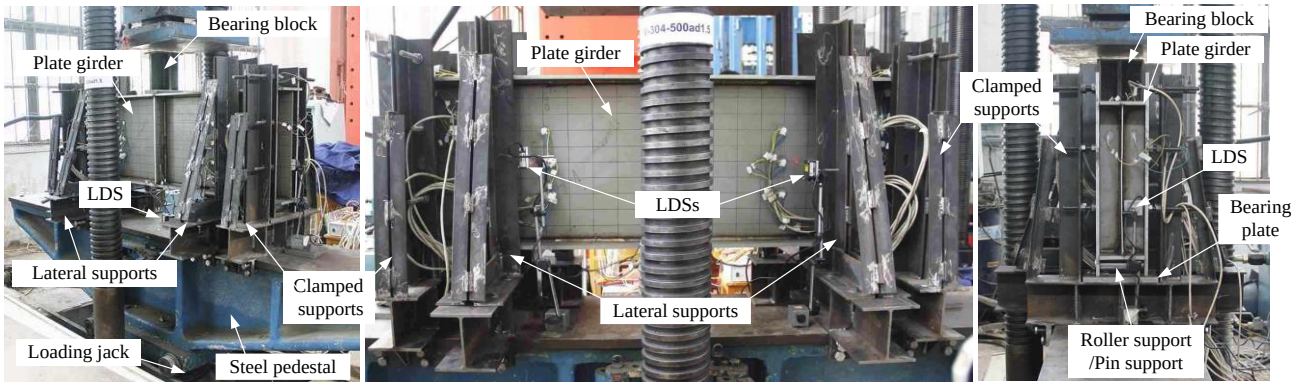

(a) Photos

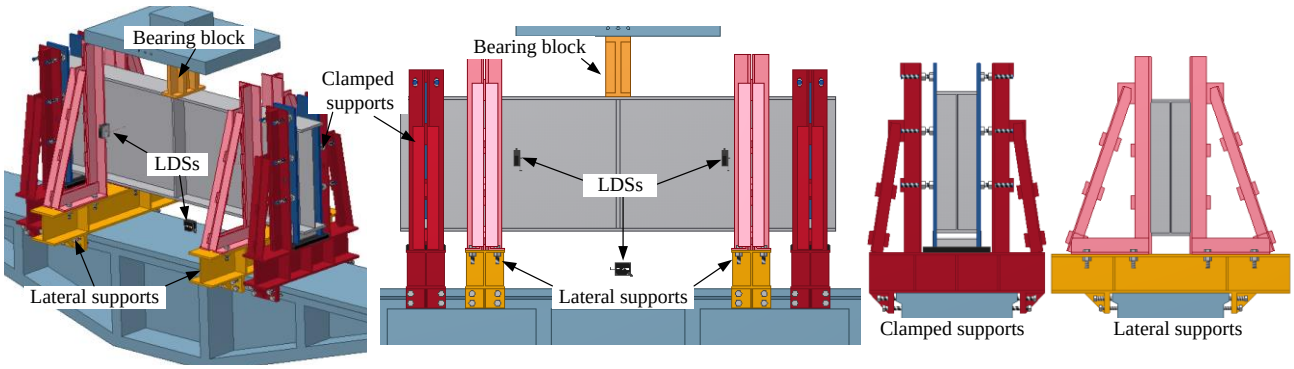

(b) Schematic drawings

Fig. 6. Test setup for shear buckling tests

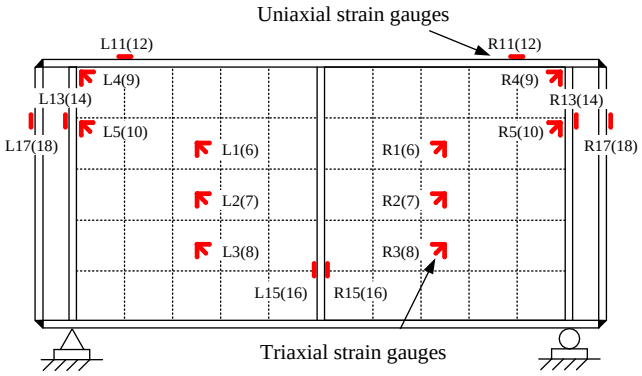

(a) Strain gauges

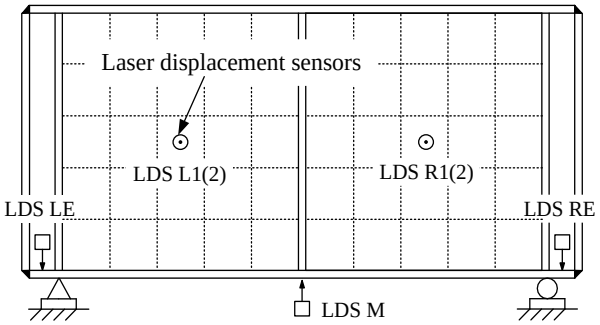

(b) Displacement transducers

Fig. 7. Instrumentation diagram for shear buckling tests

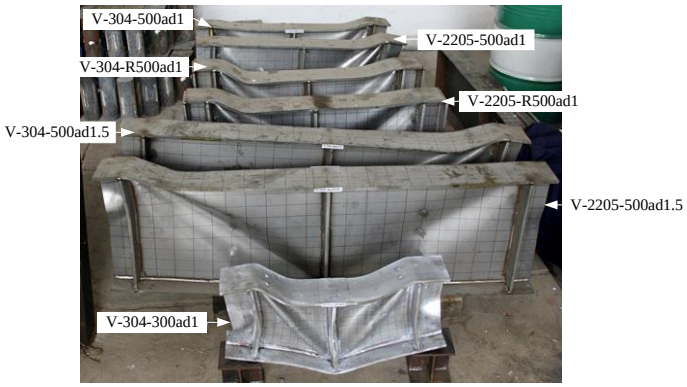

Fig. 8. Deformed shapes of the tested plate girders

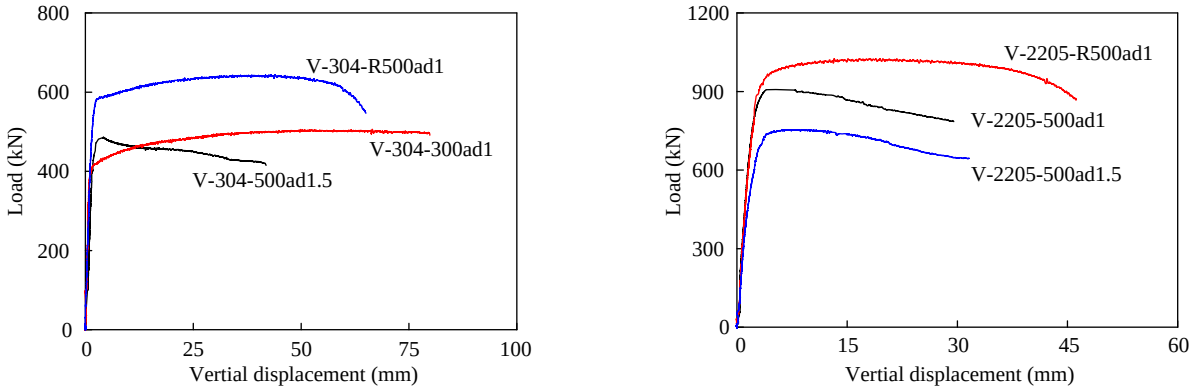

(a) Austenitic grade EN 1.4301 specimens

(b) Duplex grade EN 1.4462 specimens

Fig. 9. Load versus mid-span vertical displacement curves for tested specimens

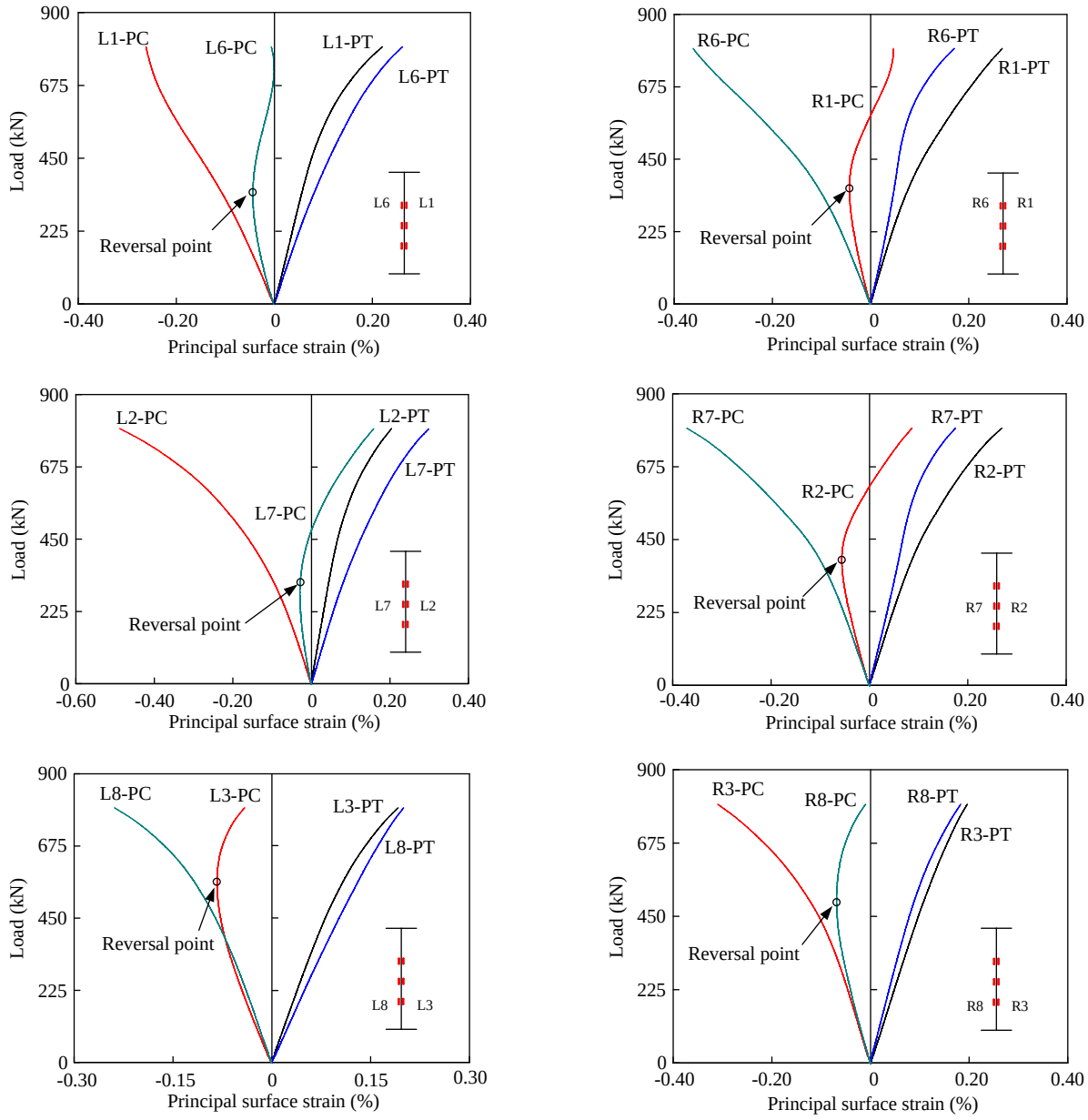

Fig. 10. Initial part of load versus principal strain curves for specimen V-2205-R500ad1

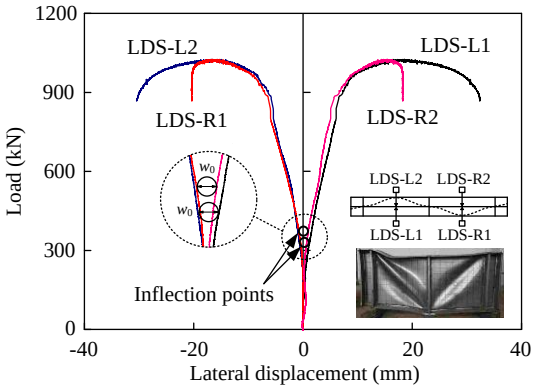

Fig. 11. Load versus lateral displacement curves for specimen V-2205-R500ad1

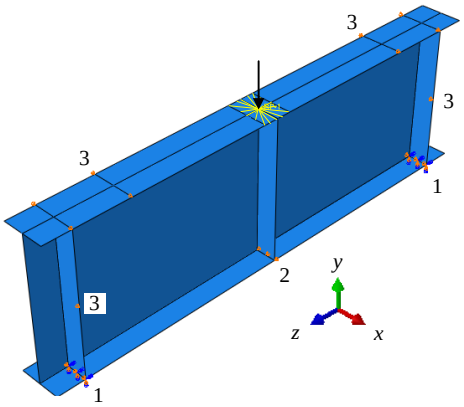

Locations	u_x	u_y	u_z	θ_x	θ_y	θ_z
1	1	1	0	0	1	1
2	0	0	1	0	0	0
3	1	0	0	0	0	0

0=free
1=restrained

Fig. 12. Boundary conditions defined in FE models

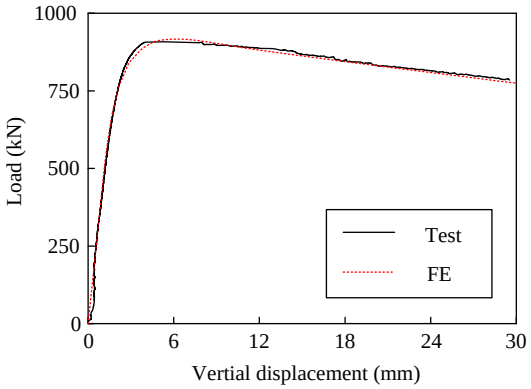

Fig. 13. Comparison between test and FE load versus vertical displacement for specimen V-2205-500ad1

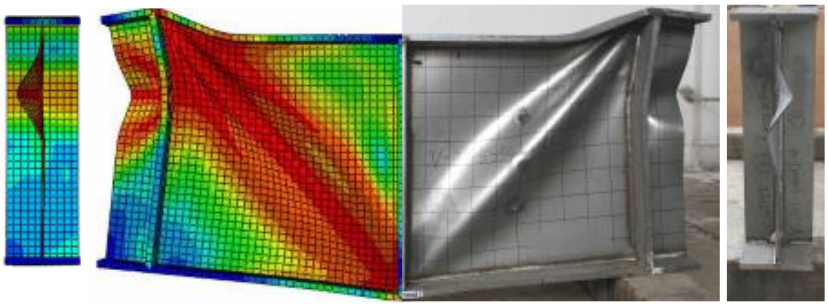

Fig. 14. Comparison between test and FE failure modes for specimen V-2205-500ad1

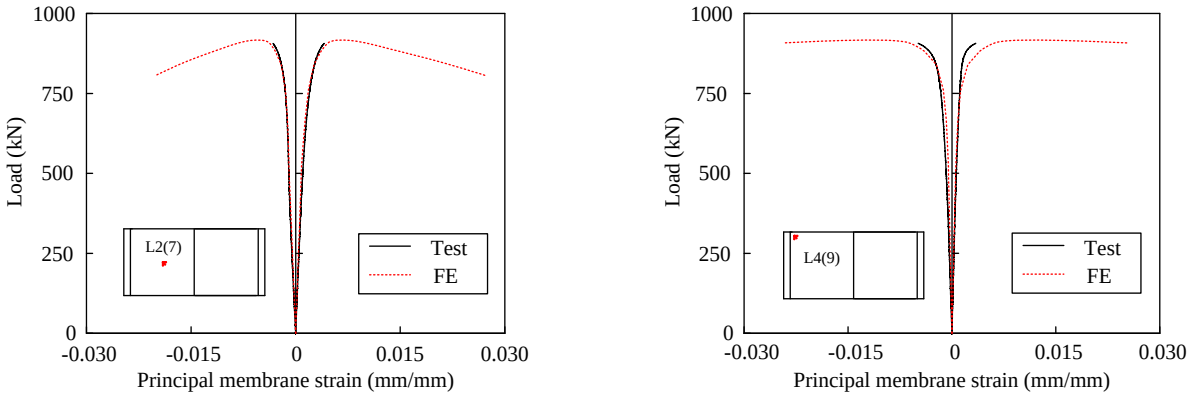

(a) At centre of web panels

(b) At upper corner of web panels

Fig. 15. Comparison between test and FE load versus principal membrane strain curves for specimen V-2205-500ad1

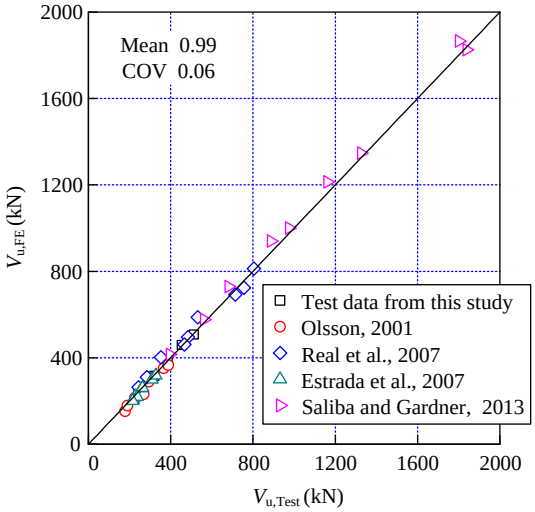

Fig. 16. Comparison of ultimate shear resistances from FE predictions and summarised tests

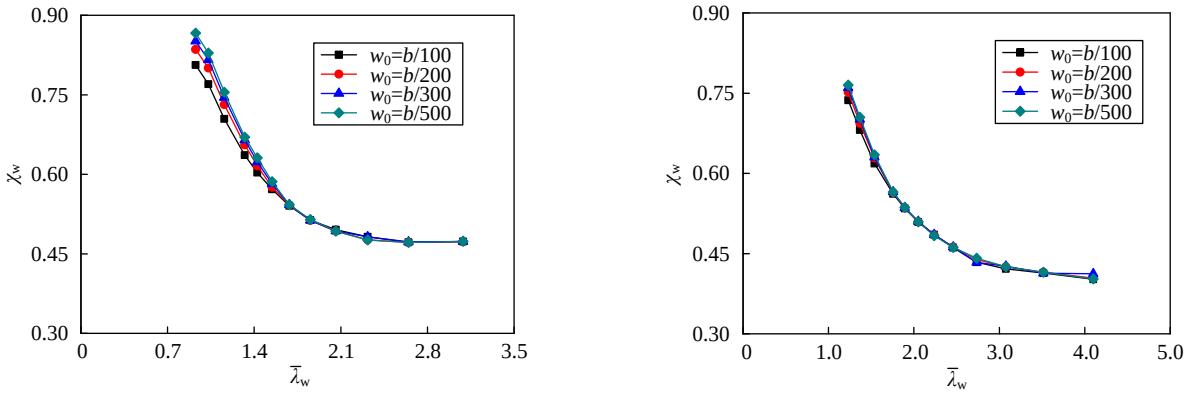

(a) Austenitic grade EN 1.4301 (b) Duplex grade EN 1.4462

Fig. 17. Influence of initial local geometric imperfection amplitude

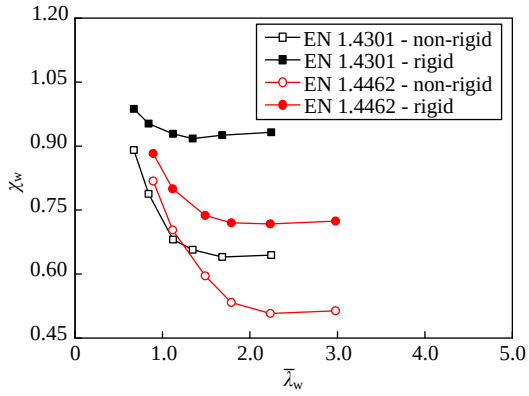

(a) $a/h_w = 0.75$

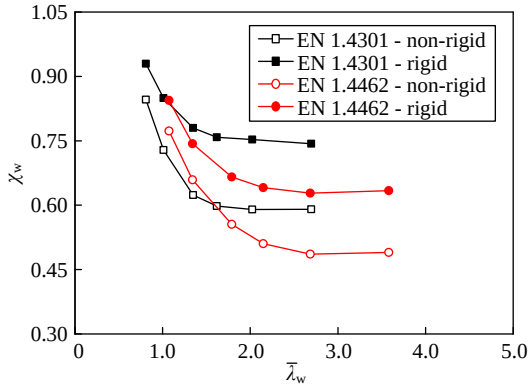

(b) $a/h_w = 1.0$

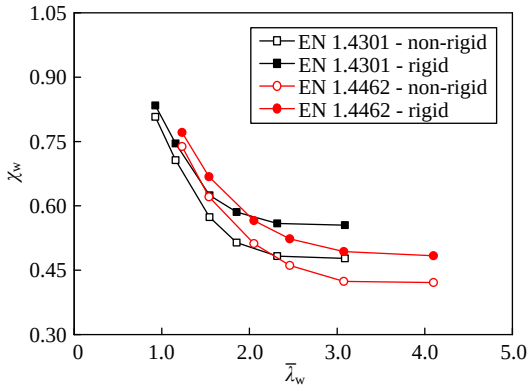

(c) $a/h_w = 1.5$

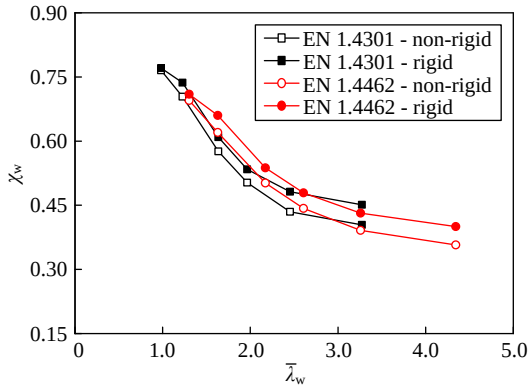

(d) $a/h_w = 2.0$

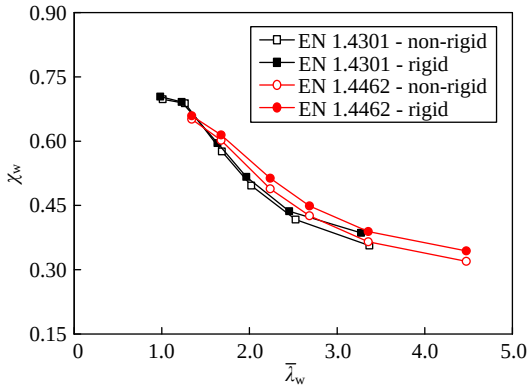

(e) $a/h_w = 2.5$

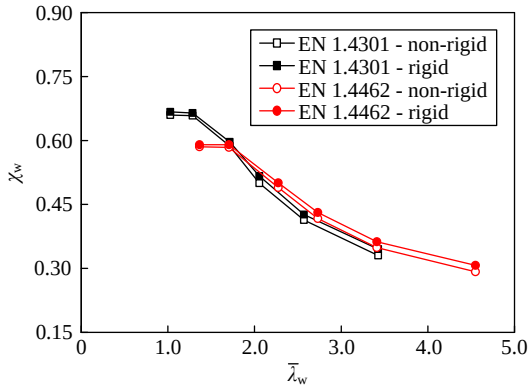

(f) $a/h_w = 3.0$

Fig. 18. Influences of aspect ratio a/h_w and end post condition

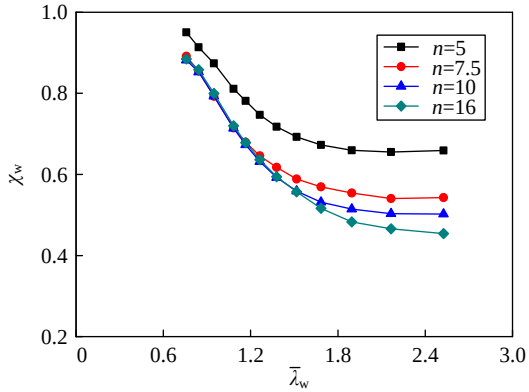

(a) $e = 0.0010$

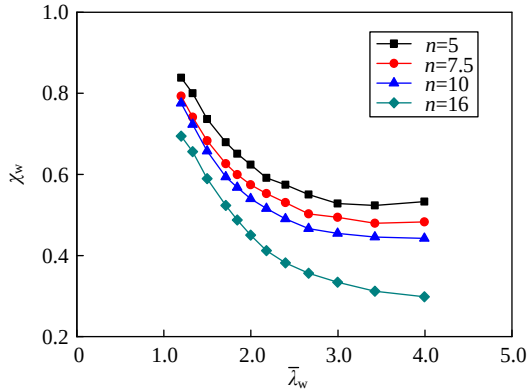

(b) $e = 0.0025$

Fig. 19. Influence of the strain hardening exponent n

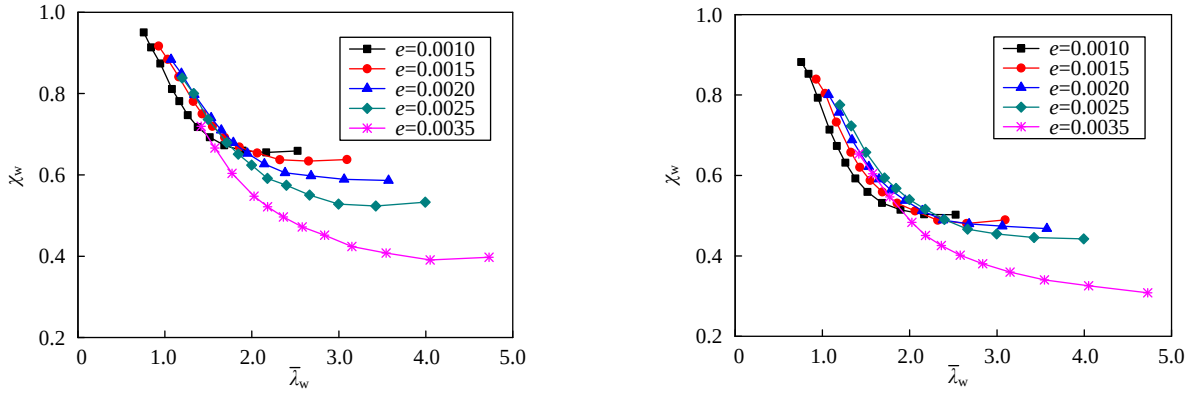

(a) $n = 5$ (b) $n = 10$

Fig. 20. Influence of the non-dimensional proof stress e

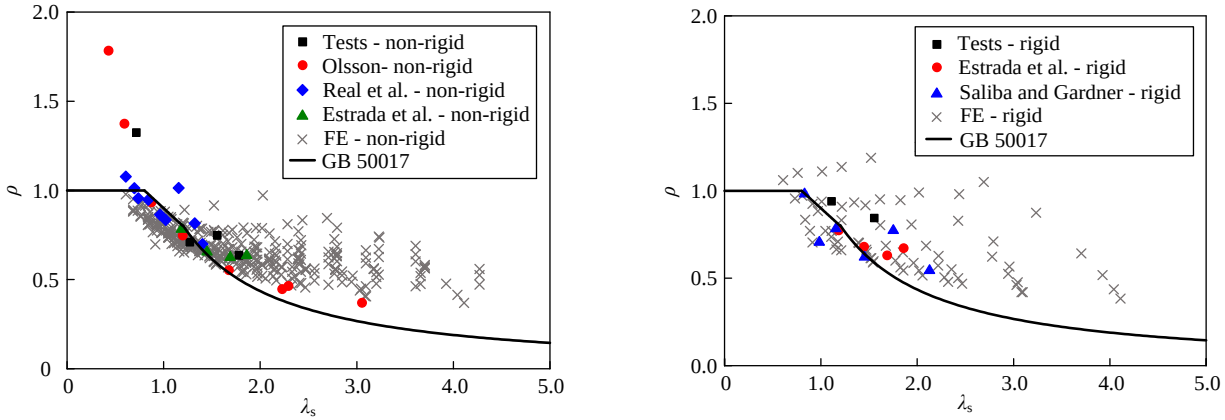

(a) Non-rigid end post (b) Rigid end post

Fig. 21. Comparison of test and FE results with GB 50017 design curves

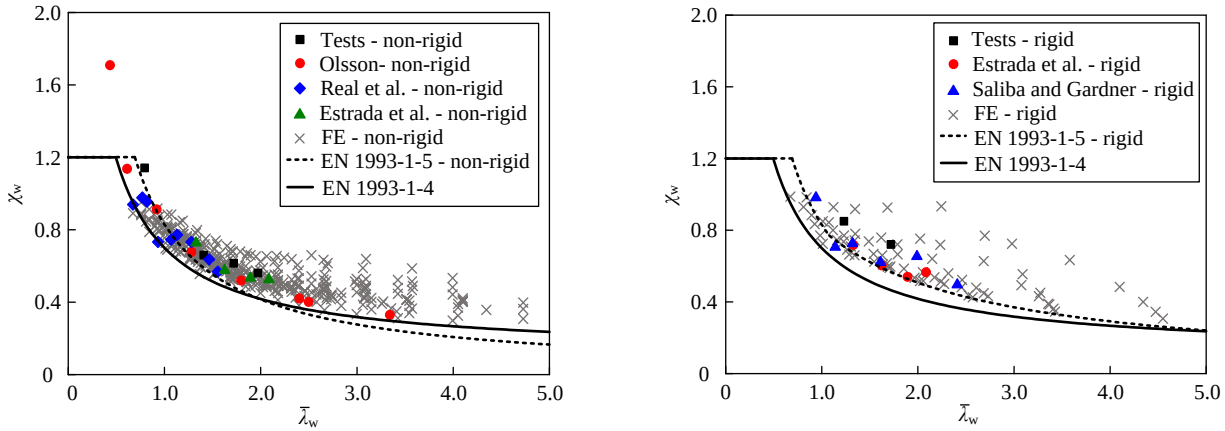

(a) Non-rigid end post (b) Rigid end post

Fig. 22. Comparison of test and FE results with EN 1993-1-5 and EN 1993-1-4 design curves

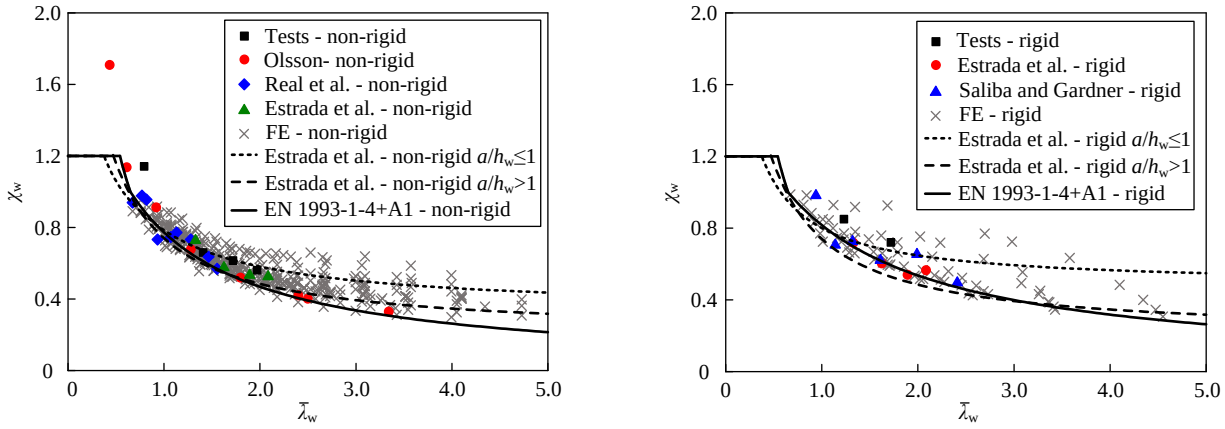

(a) Non-rigid end post (b) Rigid end post

Fig. 23. Comparison of test and FE results with design curves of Estrada et al. and EN 1993-1-4+A1

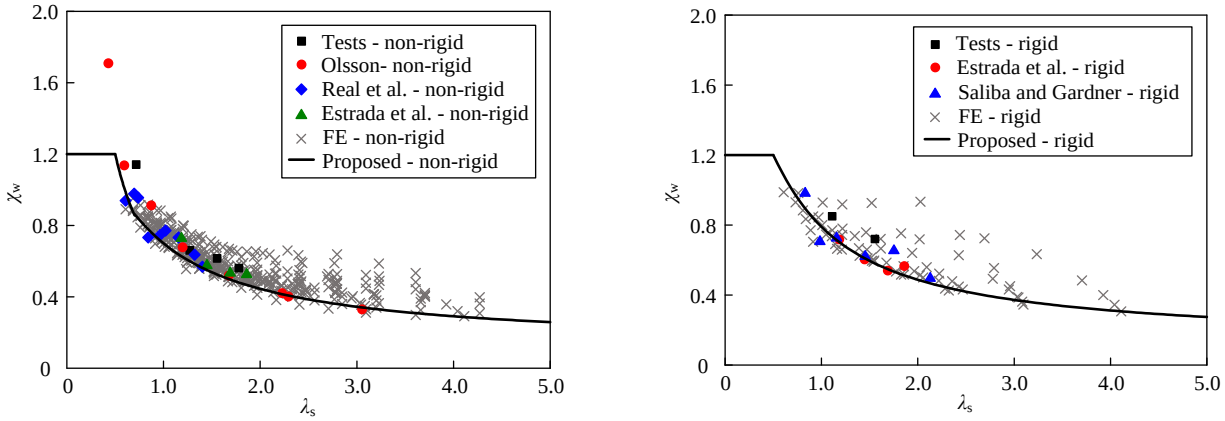

(a) Non-rigid end post (b) Rigid end post

Fig. 24. Comparison of test and FE results with proposed design curves